Available online at www.sciencedirect.com
SCIENCE DIRECT®
Journal of Photochemistry and Photobiology A: Chemistry 163 (2004) 127–134
Journal of Photochemistry and Photobiology A:Chemistry
www.elsevier.com/locate/jphotochem

Spectral properties of stilbazolium merocyanines – potential sensitizers in photodynamic therapy and diagnosis Part I. Merocyanines in model systems

Ewa Staśkowiak [a], Alina Dudkowiak [a], Izabela Hanyż [a], Krzysztof Wiktorowicz [b], Danuta Frąckowiak [a,*]

[a] *Faculty of Technical Physics, Poznań University of Technology, Nieszawska 13A, 60 965 Poznań, Poland*
[b] *Department of Biology and Environmental Sciences, Karol Marcinkowski University of Medical Sciences, Długa 1/2, 61 848 Poznań, Poland*

Received 16 October 2003; received in revised form 16 October 2003; accepted 14 November 2003

Abstract

Spectral and photochemical properties of seven stilbazolium merocyanines of different chain length and side groups attached, dissolved in ethanol or methanol solutions as well as in polyvinyl alcohol water solutions and films, were investigated. The absorption, fluorescence emission and fluorescence excitation spectra as well as steady state photoacoustic and laser induced optoacoustic spectroscopy signals were measured.

Triplet states are, because of their slow decay time, usually very effective in photochemical reaction; therefore dyes with efficient triplet states generation are suitable for destruction of illuminated diseased cells. The laser induced optoacoustic measurements were used to evaluate the efficiency of generation and decay times of dye triplet states. The quenching of the dye triplet state by oxygen was also studied.

The results show that properties of merocyanines and their interactions with macromolecules depend strongly on the type of side groups attached. The dyes with NO_2 groups attached exhibit low yield of fluorescence therefore they could be useful rather in photodynamic therapy (PDT) than for diagnostic purposes. Some of the merocyanines investigated exhibit high yields of triplet state generation and, therefore, should be effective in photodynamic reactions.

Further investigations will be carried out with the same dyes on healthy and diseased cells in order to show whether it is possible, on the grounds of spectral and photochemical properties of dye molecules in simple model systems, to predict the efficiencies of the dye incorporation into cells and the yield of photodynamic reactions.

Keywords: Energy transfer; Steady state photoacoustic spectroscopy; Laser induced optoacoustic spectroscopy; Photodynamic diagnosis; Photodynamic therapy; Stilbazolium merocyanines; Triplet states generation

1. Introduction

Stilbazolium merocyanine (Mero) dyes are promising candidates for medical applications as diagnostic and therapeutic agents [1–5] because some of them are incorporated much more efficiently into diseased than healthy cells [2,4–6]. For photodynamic therapy (PDT) and photodynamic diagnosis (PDD) the incorporation of a sensitizer into a cell has to be selective, i.e. incorporation efficiency depends on several factors, e.g. the membrane structure. The membrane structure is usually different in healthy and in diseased cells. The singlet oxygen has a lifetime of 2–5 μs in water and about 200 ns in cells (its mean free path is approximately of 45 nm). During this short time in cells, singlet oxygen can react with neighboring molecules. Therefore, the sensitizer incorporation inside the cells and a close proximity of both molecules (O_2 and dye) in the cell are so important. As it is known from model system [6–18] and stained blood cells [2–5,17] investigation, the interactions of various merocyanines with cells depends strongly on the length of Mero chain and/or the side groups attached.

When excited, as a result of illumination, in aqueous media Mero dyes can destroy cell material directly or by generation very photochemically active singlet oxygen.

Abbreviations: BCP, bromocresol purple; BPB, bromophenol blue; EtOH, ethanol; FWHM, full width at half maximum; LIOAS, laser induced optoacoustic spectroscopy; MeOH, methanol; Mero, merocyanine; PAS, steady state photoacoustic spectra; PDD, photodynamic diagnosis; PDT, photodynamic therapy; PVA, polyvinyl alcohol; TD_f, fast thermal deactivation; TD_s, slow thermal deactivation

* Corresponding author. Tel.: +48-61665-3180, fax: +48-61665-3102.
E-mail address: frackow@phys.put.poznan.pl (D. Frąckowiak).

1010-6030/$ – see front matter © 2004 Elsevier B.V. All rights reserved.
doi:10.1016/S1010-6030(03)00439-8

Both types of reactions involve the triplet states of dye [13,19–23]. Spectral properties of Mero's strongly depend on the type of microenvironment [6,7] and are changed in electric field [7–9] hence these dyes can be also applied as optical probe of membrane potential [7].

In order to select the type of Mero's most suitable for medical applications, several spectral properties such as absorption, fluorescence excitation, fluorescence and phosphorescence emission spectra as well as steady state photoacoustic spectra (PAS) and laser induced optoacoustic spectroscopy (LIOAS) signals were measured. To calculate the energy of triplet state (E_T) values the phosphorescence spectra were measured. Seven stilbazolium Mero's with different chain lengths and side groups attached, dissolved in methanol (MeOH) or ethanol (EtHO) solutions as well as in polyvinyl alcohol (PVA) water solutions and PVA films were investigated. Analysis of the signal recorded by LIOAS provides information about the yield of triplet state generation and about the decay time of triplets of Mero's investigated in the model systems used. The dyes with efficiently generated and long-lived triplet states are usually very effective in photochemistry.

The Mero dyes which, as follows from absorption and fluorescence spectra, do not enter into strong interactions with PVA polymer (an exception is Mero U*) could be promising candidates for staining the cells. Such dyes should probably be easier retained inside the cells, because they would not be able to form efficient complexes with some components of cell membrane (e.g. lipids, macromolecules). The information obtained by optical spectroscopy and photothermal spectroscopy methods should help choose the proper candidates for application in medicine. These suppositions will be tested, in further investigation, by comparing spectral properties of the dyes used, in the present work, in simple model systems with those, that will be established, for the same Mero's incorporated into healthy and diseased cells.

2. Materials and methods

The stilbazolium merocyanines were kindly provided by Dr. I. Gruda (Université du Québec, Trois-Rivières, Canada). The molecular structure and notations of the stilbazolium Mero's investigated are presented in Fig. 1 and Table 1, respectively. As follows from Table 1, the dyes investigated differ in the length of the chain (R_1) as well as types and character of R_2 and R_3 groups. It is known [1,3,8,15–17,19]

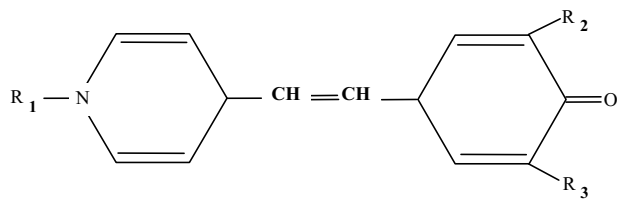

Fig. 1. Molecular structure of the merocyanine dyes investigated.

Table 1
Investigated stilbazolium merocyanines (structure is shown in Fig. 1)

	Dyes notation	R_1	R_2	R_3	Salt
1	Mero B*	$(CH_2)_{11}$–OH	H	H	HCl
2	Mero B	$(CH_2)_{11}$–OH	H	H	–
3	Mero T*	$(CH_2)_{11}$–OH	OCH_3	H	HCl
4	Mero W*	$(CH_2)_{15}$–CH_3	OCH_3	H	HCl
5	Mero U*	$(CH_2)_{11}$–H	NO_2	NO_2	HCl
6	Mero I	$(CH_2)_6$–OH	NO_2	NO_2	–
7	Mero H	$(CH_2)_6$–OH	H	NO_2	–

that these differences influence the dye interactions with a surrounding medium, dye aggregation and the orientation of the dye molecules in anisotropic media.

The solvents (MeOH and EtOH) purchased from POCH (Lublin, Poland) and the dyes, used as references in LIOAS measurements (bromocresol purple (BCP) and bromophenol blue (BPB) from RdH Laborchemikalien (Seelze, Germany)), were applied without further purification. PVA (from Aldrich) solution and isotropic films were prepared as previously [8] described.

Absorption spectra of the samples investigated were taken using a Specord M40 (Carl Zeiss, Jena, Germany) whereas the fluorescence excitation, fluorescence and phosphorescence emission spectra by means of the Fluorescence Spectrophotometer F4500 (Tokyo, Hitachi, Japan).

PAS spectra were taken using a single beam spectrometer [24]. The dye in a dry film placed in the photoacoustic cell (Model 300, MTEC Photoacoustics Inc., Ames, Iowa, USA) was illuminated by modulated light [25]. The PAS correction was made by dividing the signal obtained for the sample studied by the carbon black photoacoustic signal, making the PAS independent of the light source spectral distribution [25]. The photoacoustic signals were measured for dyes in PVA films in order to establish their interactions with polymer molecules.

The arrangement used for time-resolved photothermal measurements was a typical LIOAS apparatus [26–28]. The analysis of LIOAS signals allows a distinction between the fast thermal deactivation (TD_s) effects occurring in time shorter than the time resolution of the apparatus (about 0.5 μs) and the slow thermal deactivation (TD_s) processes which occur in longer times (up to 5 μs). The samples were illuminated by dye-nitrogen laser (flash duration, 0.2 ns). At the laser flash wavelength used the absorptions of the investigated and the reference dyes were adjusted the same. The reference dyes (BCP and BPB) in a short time exchange the whole absorbed energy into heat [26]. Two methods of LIOAS signal analysis were applied. The first one proposed by Marti et al. [29] is based on a comparison of the maximal amplitudes of the signals obtained for both investigated and reference dyes. This method provides the information on α (TD_f), thus on the part of energy which is exchanged into heat in a time shorter than the resolution time of the apparatus, and on the remaining part of non-radiative deactivation occurring slowly (TD_s). Supposing that the whole TD_s is

related to deactivation of triplet state (by the ($T_1 \sim> S_0$)) one can calculate the efficiency of triplet state generation (Φ_T) from the formula:

$$\Phi_T E_T = (1-\alpha)E_{las} - \Phi_F E_F \quad (1)$$

where α is the part of absorbed energy of the laser light (E_{las}) converted into a heat in a time shorter than the resolution time of the apparatus (which is about 0.5 μs according to the calculation proposed in [26]), Φ_F and E_F the fluorescence yield and energy of singlet state, respectively, and E_T the energy of triplet state.

The second method, proposed by Rudzki-Small et al. [30] gives the values of triplet decay times obtained by the deconvolution of the sample and reference LIOAS signals. This procedure gives reasonable results only for decay times between 0.5 and 5.0 μs. For longer decay times the results are not accurate. It is a problem for the part of the dyes investigated which do not show TD_s in this time range. For such dyes only TD_f can be estimated from LIOAS measurements by the Marti et al. [29] method.

The LIOAS signal consists of two parts: the first one related to TD of the excitation energy and the second one—to the volume changes of non-thermal origin due to sample illumination [31]. The second effect depends strongly on temperature; therefore, it is possible to evaluate its contribution by measuring LIOAS at various temperatures [30]. The LIOAS signals for some Mero dyes in alcohol solutions were measured at two temperatures at 20 and at 4 °C. The optoacoustic measurements were made also for dye solutions being in contact with air atmosphere, bubbled by nitrogen (N_2) or by oxygen (O_2). In the last case, the results were to some extent perturbed by different photochemical changes occurring in the measured and reference samples, but even in such a case the sets of results obtained for various Mero dyes can be compared.

3. Results

3.1. Absorption, fluorescence and PAS

Fig. 2 presents the normalized absorption, fluorescence excitation and fluorescence emission spectra of the dyes investigated in alcohol solutions. The Mero's B*, B, T* and W* (Fig. 2A) are soluble in EtOH solutions and Mero dyes U*, I and H (Fig. 2B) in MeOH. Concentrations of all dyes varied from 1×10^{-5} to 5×10^{-5} M and in this range of concentrations, the shapes of the absorption spectra do not change. Table 2 collects the positions and full width at half maximum (FWHM) of the main bands of absorption,

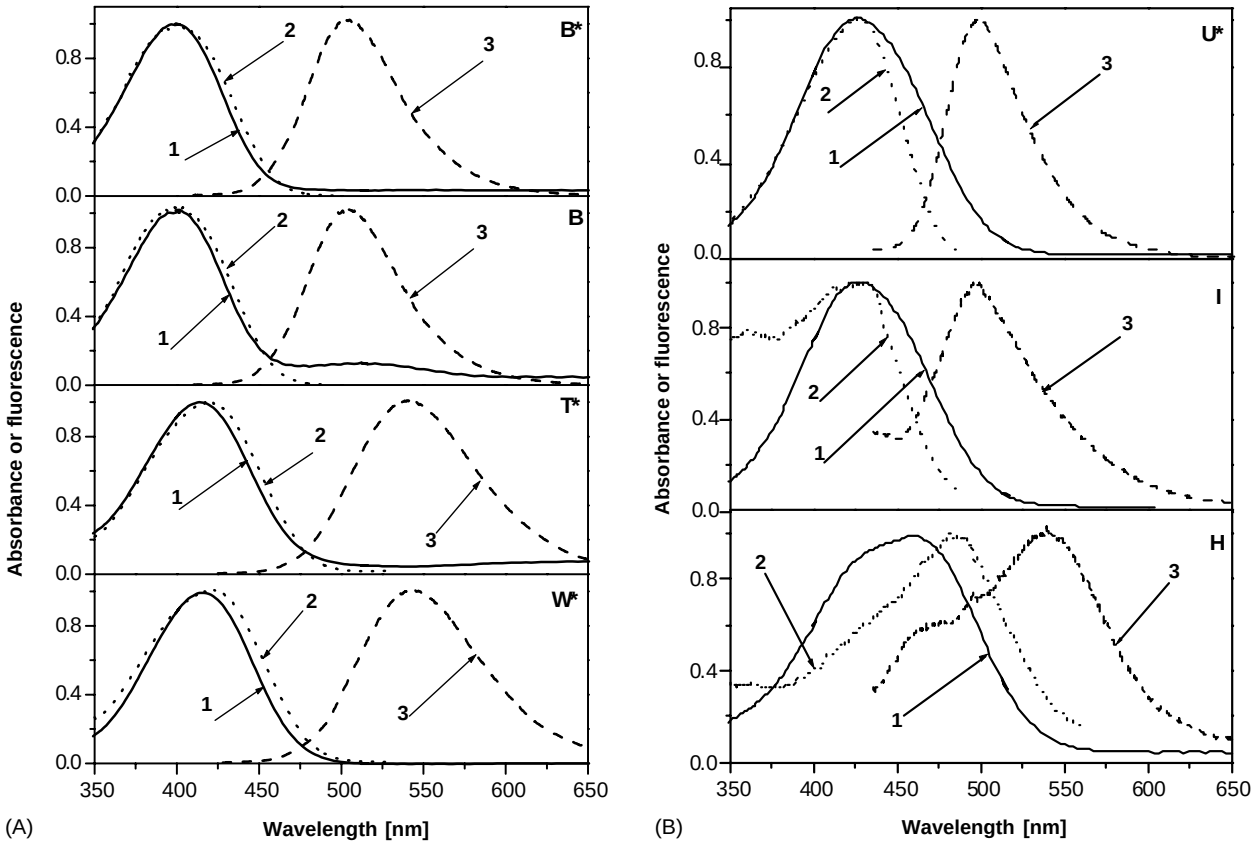

Fig. 2. Absorption, fluorescence emission and excitation spectra of the dyes in: (A) ethanol, Mero's B*, B, T*, W* and (B) methanol, Mero's U*, I, H. Curve numbers: (1) absorption; (2) fluorescence excitation; (3) fluorescence emission. Excitation wavelengths in emission spectra: B, B*: 400 nm, T*, W*: 413 nm, U*: 426 nm, I: 428 nm, H: 456 nm; observation wavelengths in excitation spectra: B*, B: 500 nm; T *, W *: 543 nm; U*, I: 498 nm, H: 538 nm.

Table 2
Spectral properties of the stilbazolium merocyanines in alcohol solvents

Dyes	A		F			F_{exc}		$\Delta\lambda_{F-A}$ (nm)
	λ_{max} (nm)	FWHM (nm)	λ_{max} (nm)	FWHM (nm)	Φ_F	λ_{max} (nm)	FWHM (nm)	
Mero B*	398	57.0	503	60.3	0.13	398	62.0	105
Mero B	398	59.4	504	60.3	0.16	399	63.0	106
Mero T*	414	64.2	543	76.4	0.30	415	68.2	129
Mero W*	414	62.9	543	75.6	0.28	415	73.9	129
Mero U*	429	75.7	500	51.0	0.01	421	62.3	71
Mero I	428	63.5	498	79.7	≈0	427	54.2	70
Mero H	459	92.1	536	86.2	≈0	483	67.2	77

(B*, B, T*, W* in ethanol; U*, I, H in methanol; concentrations order 10^{-5} M; temperature 20 °C; in contact with air atmosphere); A: absorption, F: fluorescence, F_{exc}: fluorescence excitation, FWHM: full with at half maximum, λ_{max}: wavelength at maximum, $\Delta\lambda_{F-A}$: Stokes shift, Φ_F: yield of fluorescence.

Table 3
Results of LIOAS signals analysis of the dyes in alcohols under N_2 atmosphere

	λ_{exc} (nm) LIOAS	Φ_F	α	k_1	k_2	τ_2 (μs)	λ_T (nm)	E_T (kJ/mol)	Φ_T
Mero B*	384	0.15	0.54	0.54	0.02	4.28	820	145.5	0.74
Mero B	384	0.19	0.49	0.52	0.001	4.04	820	145.5	0.80
		0.25*	0.31*	0.33*	0.05*	0.64*			≈1*
Mero T*	415	0.38	0.42	0.43	0.01	1.73	823	145.0	0.67
Mero W*	415	0.30	0.62	0.62	0.04	≪0.5	823	145.0	0.30
Mero U*	420	0.01	0.96	0.98	0.04	2.27	820	145.5	0.06
Mero I	420	≈0	0.13	0.12	0.03	1.79	746	160.0	≈1
Mero H	420	≈0	0.77	0.77	0.06	1.23	820	145.5	0.45

Temperature 20 and 4 °C for Mero B: the results with *; α and Φ_T on the basis of formula (1), k_1 preexponential factor for $\tau_1 \leq 0.5$ μs, k_2 and τ_2: preexponential factor and decay time, respectively, of the slow component obtained from deconvolution, accuracy of calculated values α, $k_{1,2}$, τ and Φ_T: about 5%, λ_{exc}, λ_T and E_T: excitation wavelength used in LIOAS measurements, phosphorescence wavelengths and triplet state energy, respectively.

fluorescence excitation and emission spectra. The Stokes shifts between fluorescence and absorption spectra are also shown in Table 2.

The relative fluorescence yields of the dyes were calculated on the basis of the comparison with the dyes of known fluorescence yield (Table 2) as well as from the fluorescence and absorption spectra (not shown). The yield values obtained by both methods were similar within the method's accuracy. The yield of fluorescence was established also for solutions in contact with O_2 and in N_2 atmosphere as well as at various temperatures. These data are necessary for estimation of the yields of dye triplet state generation in different conditions, e.g. in contact with N_2, O_2 or air atmosphere and at different temperatures. The examples of such data are given in Tables 3 and 4.

The positions of the main absorption maximum of the dyes in alcohols do not differ dramatically for the Mero's investigated, they change from 398 to 414 nm for Mero's dissolved in EtOH and from 428 to 459 nm for Mero's in MeOH. These changes are not correlated with the length of R_1 group as well as the presence of the salt (Tables 1 and 2). It depends rather on the types and donor–acceptor character of R_2 and R_3 side groups.

As follows from Fig. 2 and Tables 1 and 2, the type of the side groups attached also influences the spectral properties of Mero dyes. The Mero's investigated can be divided into two groups. The dyes from the first group are soluble in EtOH (Fig. 2A) and exhibit very similar shapes of absorption and fluorescence excitation spectra as well as similar Stokes shift equal to 105–106 nm for Mero's B, B* and to 129 nm for T*, W* (Table 2). The dyes from the second group, soluble in MeOH (Fig. 2B) exhibit different shapes of absorption and fluorescence excitation spectra and very different FWHM values of fluorescence and absorption bands as well as smaller Stokes shift (about 70–77 nm). It is clear that these dyes occur in several "forms" characterized

Table 4
The examples of LIOAS signals analysis results obtained in contact with air or O_2 atmosphere at 20 °C (description of calculated values as in Table 3)

		Temperature (°C)	λ_{exc} (nm) LIOAS	Φ_F	α	k_1	k_2	τ_2 (μs) λ_T(nm)	E_T (kJ/mol)	Φ_T	
Mero T*	O_2	20	415	0.27	0.81	0.89	0.04	3.21	823	145.0	0.02
	Air			0.30	0.50	0.50	0.03	2.27			0.56
Mero H	O_2	20	420	≈0	1.04	0.96	0.23	4.42	820	145.5	0.02
	Air			≈0	0.78	0.78	0.05	3.40			0.43

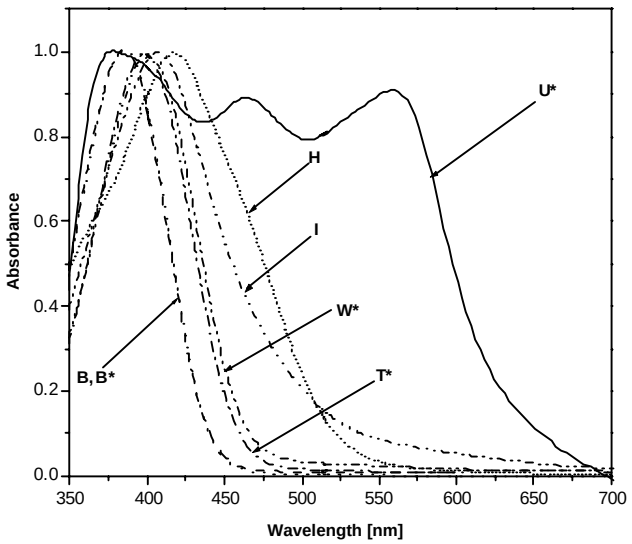

Fig. 3. Absorption spectra of the dyes in the water PVA solution.

by different fluorescence yields. These species could be created by different interactions with solvent or by mutual interaction of dye molecules. The yield of fluorescent forms of these dyes is also very low, i.e. much lower than that of the dyes from the first group (Table 2). These yields are low even in N_2 atmosphere (Table 3).

The results obtained for Mero's with NO_2 groups soluble in MeOH could suggest the presence various solvated or aggregated forms of dyes in the solution. The dependence of the dye absorbance on temperature was checked for Mero B in EtOH in the range from 4 to 20 °C. The change in dye absorbance versus temperature was very weak (about 8%). It suggests that the dyes in alcohol solutions are not aggregated in the concentration range used.

The yields of fluorescence of all Mero dyes investigated depend, of course, on the oxygen presence and temperature (Tables 2–4). A decrease in temperature causes an increase in Φ_F, whereas the presence of oxygen causes its decrease. With the determined yields of fluorescence (Tables 2–4) the efficiencies of triplet states generation were calculated, on the grounds of the formula (1) (Tables 3 and 4).

Fig. 3 shows the absorption spectra of the same set of dyes in liquid PVA water solutions. In most cases the absorption bands are slightly shifted to the blue (about 15–20 nm) in comparison to their positions in alcohols, but the shapes of the bands are similar. The exceptions are only Mero's H and U* (Fig. 3).

A different situation is observed for dyes in dry PVA films (Fig. 4).A particularly strong effect of the PVA presence in solution and in film on the absorption spectra have been observed only for Mero U* when compared to those taken in MeOH solution (Figs. 2–4). The absorption maxima of the other Mero's in PVA film are again shifted in respect to those in PVA solutions (now to the red) and the positions of the main absorption bands are similar as those observed in alcohols (Fig. 4, Table 2). In many cases the absorption and fluorescence excitation bands are somewhat mutually shifted (Fig. 4). In the case of Mero H in fluid solution of PVA, the absorption maxima exhibit some shift but the shapes of the spectra in MeOH, fluid PVA and PVA film in every case show at least the presence of two dye forms irrespective of the surroundings (Figs. 2–4).

At the light modulation used for the dyes in PVA films, the paths of thermal diffusion are much shorter than those of absorption, therefore, the PAS signal is proportional to the light absorbed converted into heat [25]. The PAS measured (Fig. 4) at the following light modulation frequencies (10, 20 and 30 Hz) showed the spectra of the same shape. For the dyes exhibiting a lower amount of TD_f (it means higher TD_s values) the deviation from the linear dependence of the photoacoustic signal versus $(2\pi\nu)^{-1/2}$ is stronger than for the dye exhibiting low TD_s. Examples are shown in Fig. 5. If a slow TD is related to long wavelength region the declination is different in various spectral regions. Fig. 5 shows that the variation of the photoacoustic signals with the light modulation provides some information about the contributions of TD_s related mainly to the dye triplet state [25]. The PAS of Mero's are different in shape then their absorption spectra (Fig. 4) which suggests that in PVA films some forms of dyes with various yields of TD are present.

As follows from the optical spectroscopy measurements of Mero's in different media, the strongest interaction with the polymer is observed for Mero U*. Mero U* because of its strong interaction with the polymer in solution as well as in film, seems to be unsuitable for staining the cell. It is difficult to explain why Mero U* shows such a strong interaction with the polymer. On the basis of the optical spectroscopy measurements for the whole set of Mero's we can exclude the influence on this interaction of the following: (1) the presence of the salt (no difference observed for Mero's B and B*); (2) the attachment of NO_2 groups in position R_2 and R_3 (from a comparison of Mero's U* and I); (3) the lengths of the Mero chain (e.g. from the spectra of Mero's T* and W*).

3.2. LIOAS results

The typical waveform signals for the dye and the reference samples are shown in Fig. 6. The data obtained from analysis of LIOAS signals measured for Mero's in alcohols in contact with N_2, O_2 and air atmosphere are given in Tables 3 and 4. The parts of TD_f energy (α) were estimated on the grounds of the Marti et al. [29] method. The preexponential factors (k_1 and k_2) and decay times τ_2 of TD_s component were obtained by the Rudzki-Small et al. deconvolution [30]. Finally, the efficiency of the triplet state generation (Φ_T) was also from the formula (1) (Tables 3 and 4). For Mero B, the results obtained at lower (4 °C) temperature are gathered in Table 3. The presence of oxygen in the samples being with contact with air or bubbled by pure oxygen, changes the LIOAS results and also the Φ_T values. The examples of such results are shown in Table 4.

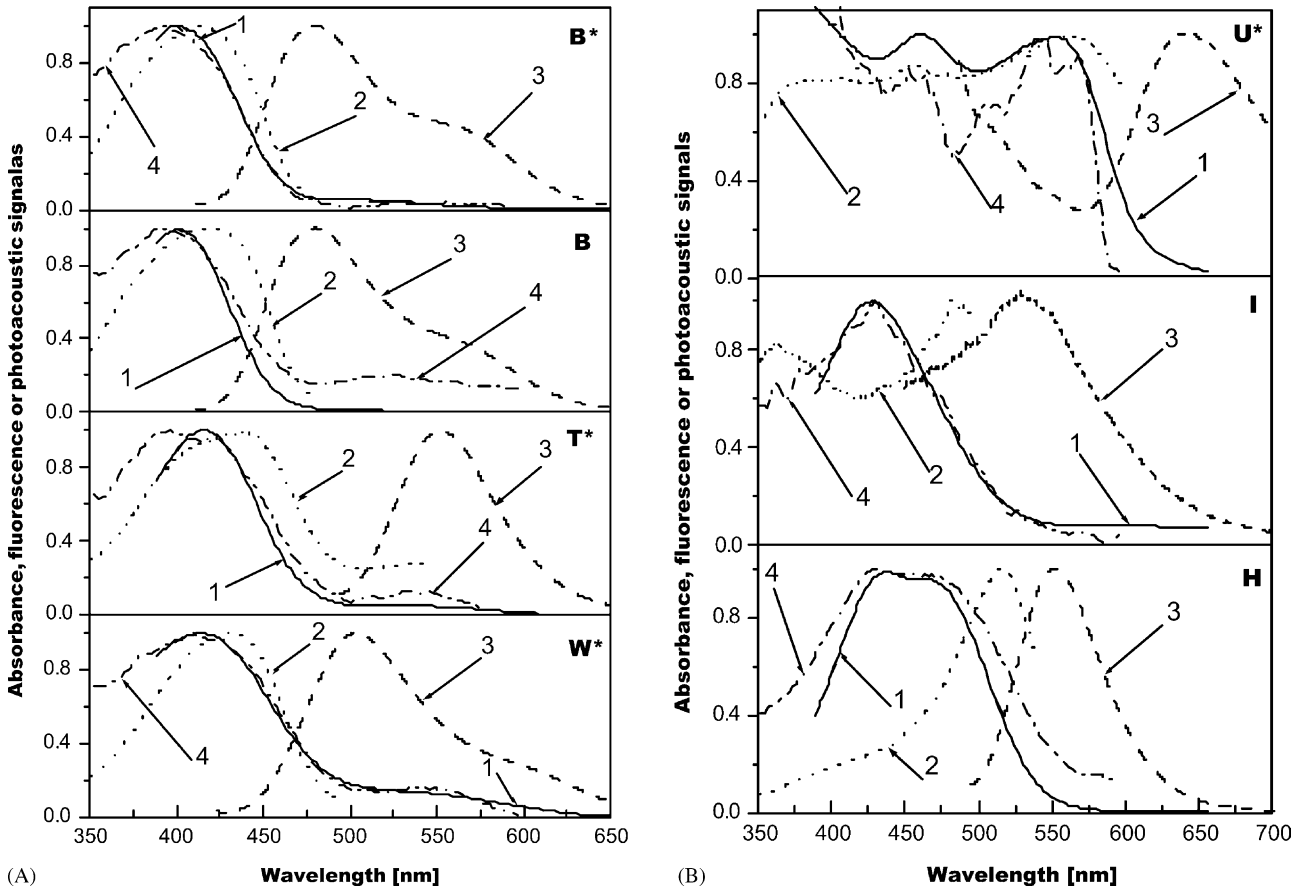

Fig. 4. Absorption, fluorescence excitation and emission, PAS spectra of the dyes in the PVA film: (A) Mero's B*, B, T*, W* and (B) Mero's U*, I, H. Curve numbers: (1) absorption; (2) fluorescence excitation; (3) fluorescence emission; (4) PAS. Excitation wavelengths in emission spectra: B, B*: 400 nm, T*, W*: 412 nm, U*: 459 nm, I: 428 nm, H: 469 nm; observation wavelengths in excitation spectra: B*, B: 480 nm; T *: 550 nm, W*: 502 nm; U*: 641 nm, I: 528 nm, H: 552 nm.

As follows from a comparison of Φ_T values in Table 4 with those in Table 3, the pure oxygen significantly quenches the dye triplets, whereas a decrease in temperature causes an increase in Φ_F and a decrease in α (e.g. Mero B). The effect of temperature for different samples is different and probably related to the effect of temperature on the volume of dye–solvent complexes [31]. The highest yields of triplet generation calculated from the measurements at

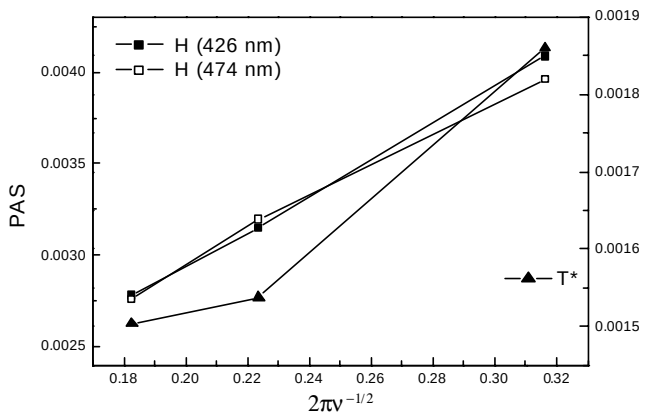

Fig. 5. Dependence of the photoacoustic signals at maxima of PAS for Mero's H and T* in the PVA film on $(2\pi\mu)^{-1/2}$ (ν, frequency of light modulation).

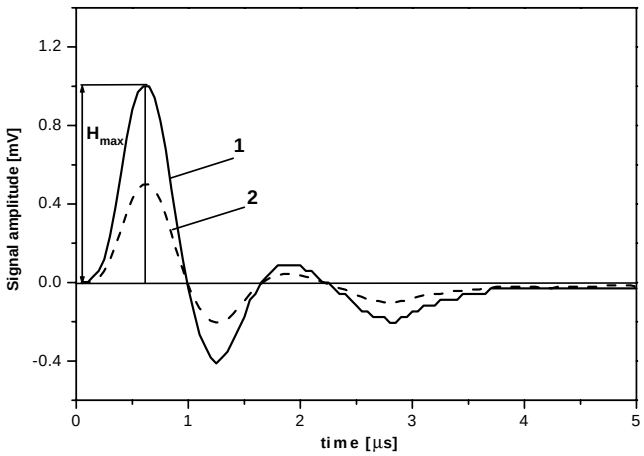

Fig. 6. Example of the LIOAS waveform signal measured in air atmosphere: curve 1: BCP (reference); curve 2: Mero T* (sample).

room temperature and under N_2 atmosphere is for Mero's I and B, but this yield it is also relatively high for Mero's T* and B*. In all Mero's investigated the pure oxygen strongly quenched their triplet states, but the influence of atmospheric concentration of O_2 is not so dramatic and is comparable with effects observed under N_2 atmosphere (Tables 3 and 4).

From Table 3 it follows that α (k_1) takes the highest value for Mero U* and the lowest for Mero I (both with two NO_2 groups). The values of τ_2 and k_2 related to TD_s components are comparable for all Mero's with NO_2 group (U*, I, H) as well as for Mero T*. The longest time decays (τ_2) show Mero's B, B* and the shortest–Mero W*. In N_2 atmosphere the relatively high Φ_T values are obtained for Mero's B, B*, T* and I. From this group of dyes, the lowest quenching of triplet state by O_2 is observed for Mero B and B* (Φ_T about 0.26 in O_2). This result shows that even at an excess amount of O_2 the triplet states of those Mero's are still able to participate in photodynamic reaction. It is important also that the Mero's (showing high Φ_T values) have also long decay times of triplet states in the presence of oxygen (Table 4), which indicates a possibility of the dye interaction with oxygen and the formation of reactive singlet oxygen by triplet energy transfer. The effect of quenching of the dye triplet states (Table 4) accompanied by a decrease in Φ_F as well as an increase in τ_2 values and a parallel increase in TD_f processes (values of α (k_1) increase) have been observed for all Mero's. The opposite effect is observed with lowering temperature (Table 3).

The photochemical properties obtained from LIOAS analysis are difficult to correlate with the chemical structure of the Mero dyes. It seems that the method of optical spectroscopy and photothermal spectroscopy methods are complementary and they can find application in selection of the dyes for medical photodynamic treatment.

On the basis of the results presented in Figs. 2–6 and Tables 2–4, the Mero's B, B*, T* and I because of their spectral and photochemical properties (high Φ_T) can be applied as promising sensitizers to stain the blood cells in further experiments. As follows from a comparison of the spectral properties of the dyes in fluid and rigid PVA and in alcohol solutions the interactions of various Mero's with macromolecular chains are much different and depend on the medium fluidity and the polymer presence. It is expected that these dyes could enter into different interactions with various components of cells and cell membranes. In general, it is anticipated to establish the influence of some side groups (H, OCH_3 and NO_2) attached to stilbazolium Mero's on the selectivity and efficiency of the dye incorporation into diseased and healthy cells and, of course, on the photodynamic reaction yield in stained cells. We hope also to find out whether it is possible to make preliminary selection of proper dye-senstizers for PDT and PDD on the basis of their spectral and photochemical properties in simple model systems. It seems that a combination of the optical spectroscopy and photothermal methods can provide valuable information for possible selection of dyes useful in medicine.

Acknowledgements

This work was supported by Polish Committee for Scientific Research (grant no. 3 P05B 073 24, 2003-2005) (for A.D., E.S. and K.W.) and by Interuniversities grant (no 502-4-90-17) (for D.F.), Poznań University of Technology (grant 62-176/03-DS) (for I.H.).

References

[1] D.P. Valentzano, Photochem. Photobiol. 46 (1987) 147.
[2] I. Gruda, M. Page, F. Bolduc, S. Laliberte, C. Noel, Anticancer Res. 7 (1987) 1125.
[3] S. Laliberte, I. Gruda, M. Page, F. Garnier, A. Pepin, C. Noel, Anticancer Res. 10 (1990) 939.
[4] D. Frąckowiak, K. Wiktorowicz, J. Cofta, M. Niedbalska, M. Latosińska, Acta. Biochim. Polon. 42 (1995) 61.
[5] K. Wiktorowicz, M. Niedbalska, A. Planner, D. Frąckowiak, Acta Biochim. Polon. 42 (1995) 333.
[6] D. Frąckowiak, M. Niedbalska, M. Romanowski, I. Gruda, Stud. Biophys. 123 (1988) 135.
[7] D. Frąckowiak, M. Romanowski, S. Hotchandani, L. LeBlanc, R.M. Leblanc, I. Gruda, Bioelectrochem. Bioenerg. 19 (1988) 371.
[8] D. Frąckowiak, I. Gruda, M. Niedbalska, M. Romanowski, A. Dudkowiak, J. Photochem. Photobiol. A 54 (1990) 37.
[9] J. Goc, D. Frąckowiak, J. Photochem. Photobiol. A 59 (1991) 233.
[10] I. Gruda, S. Hotchandani, D. Frąckowiak, Photobiochem. Photobiophys. 12 (1986) 267.
[11] N.S. Naser, A. Planner, D. Frąckowiak, J. Photochem. Photobiol. A 113 (1998) 279.
[12] T. Martyński, T. Teteishi, J. Miyake, A. Ptak, D. Frąckowiak, Thin Solid Films 306 (1997) 154.
[13] A. Planner, D. Frąckowiak, J. Photochem. Photobiol. A 140 (2001) 223.
[14] J. Łukasiewicz, M. Hara, Ch. Nakamura, J. Miyake, D. Wróbel, D. Frąckowiak, J. Photochem. Photobiol. A 138 (2001) 235.
[15] N.S. Naser, A. Planner, D. Frąckowiak, Acta Phys. Polon. A 42 (1997) 535.
[16] I. Gruda, S. Laliberte, M. Niedbalska, D. Frąckowiak, J. Luminescence 39 (1987) 1.
[17] D. Frąckowiak, A. Balter, J. Szurkowski, L. Lorrain, B. Szych, S. Hotchandani, Acta. Phys. Polon. A 74 (1988) 125.
[18] A. Ptak, A. Der, R. Toth-Boconadi, N.S. Naser, D. Frąckowiak, J. Photochem. Photobiol. A 104 (1997) 133.
[19] A. Mishra, R.K. Behera, P.K. Behera, B.K. Mishra, G.B. Behera, Chem. Rev. 100 (2000) 1973.
[20] A. Seret, M. Hoebeke, A. Van de Vorst, Photochem. Photobiol. 52 (1990) 601.
[21] M. Hoebecke, J. Photochem. Photobiol. B 22 (1994) 229.
[22] M. Hoebecke, A. Van de Vorst, Photochem. Photobiol. 61 (1995) 347.
[23] F. Aramendia, M. Krieg, C. Nitsch, E. Bittersmann, S.E. Braslavsky, Photochem. Photobiol. 48 (1988) 187.
[24] D. Duchame, A. Tessier, R.M. Leblanc, Rev. Sci. Instrum. 50 (1979) 1461.
[25] A. Rosencwaig, Photoacoustics and photoacoustic spectroscopy, in: P.J. Elving, J.D. Winefordner (Eds.), Wiley, New York, 1980, pp. 57–69.

[26] S.E. Braslavsky, G.E. Heibel, Chem. Rev. 92 (1992) 1381.
[27] A. Bartczak, Y. Namiki, D.J. Quian, J. Miyake, A. Boguta, J. Goc, J. Łukasiewicz, D. Frąckowiak, J. Photochem. Photobiol. A 159 (2003) 259.
[28] D.J. Quian, A. Planner, J. Miyake, D. Frąckowiak, J. Photochem. Photobiol. A 144 (2001) 91.
[29] C. Marti, S. Nonell, M. Nicolaus, T. Torres, Photochem. Photobiol. 71 (2000) 53.
[30] J. Rudzki-Small, L.J. Libertini, E.W. Small, Phys. Chem. 42 (1992) 29.
[31] T. Gensch, S.E. Braslavsky, J. Phys. Chem. B 101 (1997) 101.